Colloidal Motor

International Edition: DOI: 10.1002/anie.201509978
German Edition: DOI: 10.1002/ange.201509978

Directed Self-Assembly Pathways of Active Colloidal Clusters

*Jie Zhang, Jing Yan, and Steve Granick**

Abstract: *Despite the mounting interest in synthetic active particles, too little is known about their assembly into higher-order clusters. Here, mixing bare silica particles with Janus particles that are self-propelled in electric fields, we assemble rotating chiral clusters of various sorts, their structures consisting of active particles wrapped around central "hub" particles. These clusters self-assemble from the competition between standard energetic interactions and the need to be stable as the clusters rotate when the energy source is turned on, and fall apart when the energy input is off. This allows one to guide the formation of intended clusters, as the final structure depends notably on the sequence of steps in which the clusters form.*

Many interesting instances of self-assembly take place in the presence of motion under controlled external fields (shear,[1] electric,[2] magnetic[3]) and more complicated chemical fields such as in biological entities,[4] so that it becomes a problem of reaching steady-state, necessarily outside equilibrium, and even more importantly of doing so in a rationally directed fashion. How to design and direct the assembly of elements with autonomous motion into higher-order structures comprises an unsolved problem with relevance from biology[5] to technology.[6] Without downplaying the important differences between such systems, it is fair to note that progress has been impeded by the paucity of experimental systems in which direct, quantitative, controlled studies are possible.

Here we investigate self-propelled particles large enough to be observed in an optical microscope with image analysis of large statistical datasets. We use a mixture of micron-sized silica particles and half-metal coated Janus particles that interact owing to the electric-field-induced dipoles.[7] They sediment at the bottom of sample cells in water and the Janus particles "swim" on the plane perpendicular to the applied AC electric field.[8] A sketch of the experimental setup is shown in Figure S1 of the Supporting Information (SI). For silica particles, the applied AC electric field induces one dipole in the center, and for Janus particles, the field induces one dipole on the metal-coated hemisphere and another dipole of different magnitude on the silica hemisphere,[9] both of them shifted from the geometrical center of the sphere (see SI for detailed calculations), creating anisotropic interactions between particles. On the other hand, Janus particle "activity," controlled by applied voltage, modulates the structure formation as well.

First we choose to work with a mixture of 3 μm Janus particles and 4 μm silica particles with a number ratio of 5:1 and a surface area coverage of 0.3 to ensure an excess of Janus particles. Janus particles are slightly attracted to the substrate due to the asymmetric flow around them,[8b] whereas pure-silica particles enjoy relatively more freedom in the direction perpendicular to the substrate. As induced dipoles are repulsive when their connection is perpendicular to the electric field but attractive when aligned with the field, we tune the field so that in-plane repulsion between a silica particle and a Janus particle turns to out-of-plane attraction when the pure-silica particle is lifted up despite its tendency to sediment (Figure 1 a).

When attraction between the pure-silica and the Janus particles overcomes the inherent repulsion between the Janus particles themselves, chiral clusters are generated in which the dynamically assembled elements rotate, either clockwise or counterclockwise, with the pure-silica particles as hub. Both tetrahedral (assembled at high activity) and square pyramidal (assembled at low activity) rotors are obtained in nearly pure form. There is no chiral preference at present but methods to consider doing so if desired have been proposed and demonstrated.[10] Representative microscope images of multiple tetrahedral and pentamer clusters are shown in Figure 1 a, below a schematic illustration of the forces that drive their formation. Supplementary Movies 1 and 2 illustrate their formation. When the hub particle size is increased from 4 μm to 6 μm in diameter, pentamers and hexamers are selected instead at high and low activities, respectively, but when the hub particle is the same size (3 μm), only tetramers form (Figure 1 b).

Figure 2 a summarizes the assembly pathways of the stable rotating tetramer and pentamer rotors assembled from 4 μm pure-silica particles and 3 μm Janus particles. They form three coexisting metastable intermediate structures consisting of a hub particle enveloped by active Janus particles, the latter with moving heads pointing toward the hub particle since active Janus particles must move toward the hub to attach. Either two or three Janus particles may attach to the hub particle all at once or one by one, as indicated by the arrows in Figure 2 a.

The tetrahedra assembled from fast-moving particles adjust to the stable rotating configuration quickly and generate a dynamic shield by rotating rapidly: during the period of one rotation, the fourth Janus particle has insufficient time to join in, although there would be space to do so, whereas the tetrahedra assembled from slow moving particles

[*] J. Zhang, Dr. J. Yan, Prof. S. Granick
Department of Materials Science and Engineering
University of Illinois
Urbana, IL 61801 (USA)
E-mail: sgranick@ibs.re.kr
Prof. S. Granick
IBS Center for Soft and Living Matter, UNIST
Ulsan 689-798 (South Korea)

Supporting information for this article can be found under http://dx.doi.org/10.1002/anie.201509978.

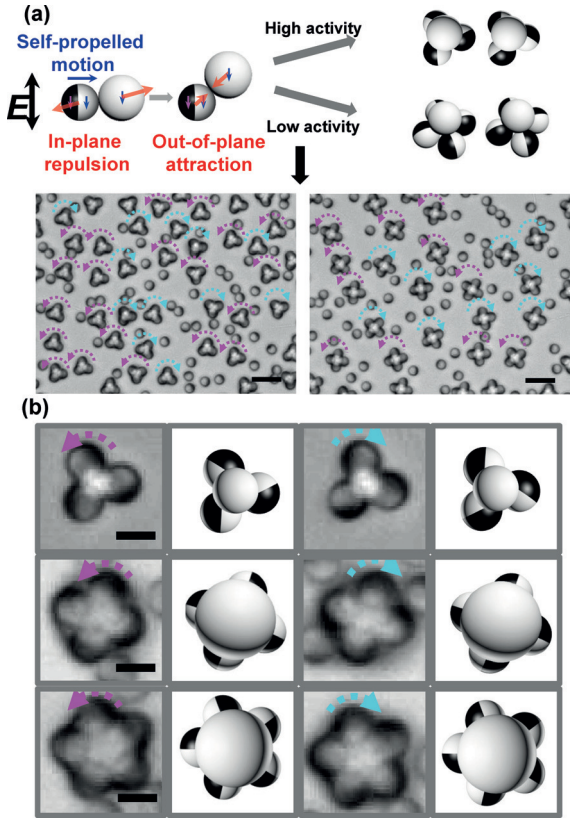

Figure 1. Directed self-assembly of chiral colloidal active clusters. Here the Janus particles are 3 μm in diameter and the diameter of the pure-silica hub particle is varied. a) With AC electric field (40 kHz), the scheme shows that one inert (pure-silica) particle is lifted slightly from the bottom of the sample cell to allow attraction of either three or four Janus active particles, resulting in tetrahedral rotors ("low activity", electric field 40 $V\,mm^{-1}$) or square pyramidal rotors ("high activity", 80 $V\,mm^{-1}$). Microscope images show these multiple clusters accompanied by unattached Janus particles whose abundance is in excess. Magenta and cyan arrows indicate counterclockwise and clockwise rotation, respectively, of the clusters in this image and below. Scale bars are 10 μm. b) Representative microscope images, paired with schematic illustrations for each of them, of the clusters for hub particles with diameter 3 μm (first row) and 6 μm (second row with high activity, 80 $V\,mm^{-1}$; third row with low activity, 40 $V\,mm^{-1}$). Scale bars are 3 μm.

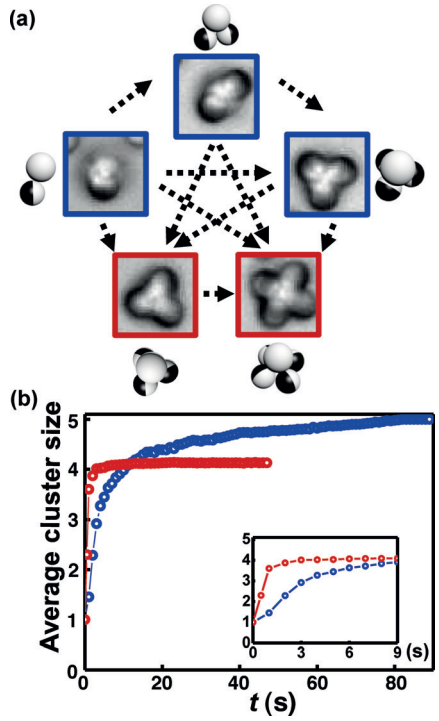

Figure 2. Assembly pathways and dynamics for 4 μm diameter bare-silica particles and 3 μm diameter Janus particles in excess abundance. a) Microscope images, each accompanied by a schematic illustration, of kinetic pathways during growth to the final configurations. Arrows denote observed structural interconversions. b) Average cluster size plotted against time as clusters grow (40 kHz electric field) at low and high activity (blue: 40 $V\,mm^{-1}$, red: 80 $V\,mm^{-1}$). Inset magnifies the first 9 s after electric field was applied.

are more floppy. Figure 2b plots the average cluster size against time, showing rapid organization into tetramers whose fast rotation (at 80 $V\,mm^{-1}$ AC electric field) leaves too little time for insertion of an additional nearby free particle; the few exceptions are those few pentamers assembled from the start when occasionally four Janus particles join the rotor before it reaches steady rotation. But when swimming is slower (40 $V\,mm^{-1}$), particles have more time to interact so that as geometry and interaction energy allow, all hub particles find their four vanes eventually. As a control experiment, after assembly at low activity, the rotation speed of pentamer rotors can be raised to a state of high swimming speed without reverting to tetrahedra, but tetrahedra formed at high activity grow into pentamers when their speed is lessened. This capability to capitalize upon organizational redundancy is an attractive design principle by which to engineer the intended structure.

As clusters grow, orientation-dependent interactions between particles begin to matter. In this system the induced dipole energy largely exceeds hydrodynamic interactions, so we only consider the induced dipole interactions for the calculation of cluster energy. A justification can be found in the SI. The energetic stabilities of tetrahedron and pentamer clusters were calculated (Figure 3): hugely larger than thermal energy, the relative changes between clusters of different size and different arrangement are subtle and independent of the electric field strength, even though experimentally, the electric field strength has a significant effect by influencing the swimming activity. The lowest-energy structures are not observed as the pathways toward them are not accessible; Janus particles swim with their dielectric sides toward the hub particles to which they are attracted. The arrows in Figure 3 indicate the experimentally observed configurations, which are neither global nor local minima, showing the failure of using only energy criteria to predict structures. Note that the actual energy landscape with each Janus particle freely rotating is much more complicated; here the curve is only shown for a special case when all participating Janus particles are rotating the same angle from the starting position based on the symmetry argument.

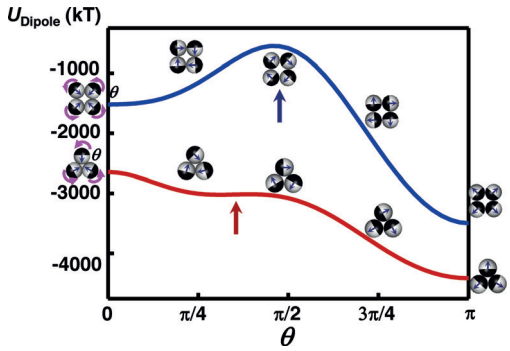

Figure 3. Calculated induced dipole energy for a tetrahedron and a pentamer (square pyramid) cluster, at 40 kHz, 80 V mm^{-1} electric field, comparing different Janus particle orientations (θ) on the *x*-axis. Hub particles are not shown in the illustrations. Regardless of the cluster size, all Janus particles are set to rotate in the same chiral direction, counterclockwise in the example drawn here, with rotation amplitude the same angle θ from the starting configuration. Arrows indicate the average observed experimentally for each of these clusters.

The most stable rotating configurations require rotational symmetry and no relative orientation change between neighboring Janus particles as the cluster rotates. For the tetramer and pentamer rotors here, Figure 4a shows the steady-state configurations of their Janus particles. The single-particle velocity in a pentamer is tangent to the trajectory of the cluster itself, whereas the velocity of particles in a tetrahedron has an additional component inward. This may help to stabilize the tetrahedron architecture. Note also that the pentamers have a larger footprint. The ideal radii of their circular orbits, as they rotate clockwise or counterclockwise, depend predictably on a simple geometric calculation (Figure 4a).

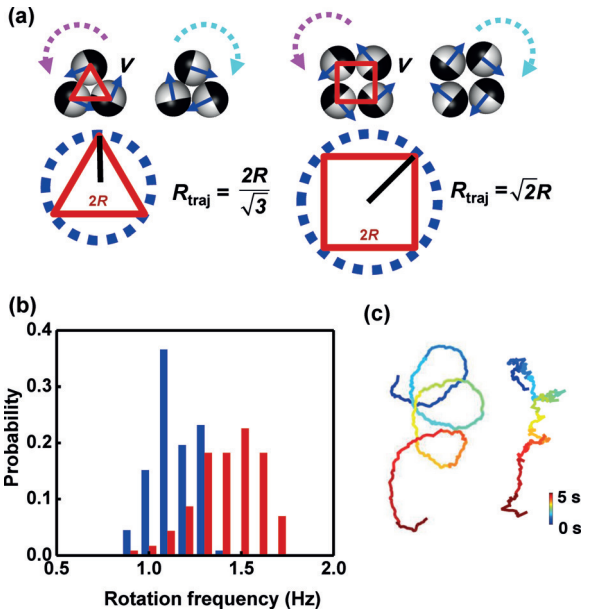

Figure 4. a) Schematic diagram showing the Janus particle orientations in the most stable rotating clusters that were experimentally observed. As indicated by the dotted blue circles below, ideally clusters would rotate in circles whose radius depends mathematically on the particle radius as shown. b) The observed probability distribution of rotation frequency is plotted against rotation frequency for tetramers (red) and pentamers (blue), for the experimental condition of 40 kHz, 80 V mm^{-1}. c) Illustrative spiral trajectory of one petal (left) and diffusional trajectory of the center (right) of a pentamer rotor.

But inevitably, in the colloid-sized world, there is all sort of randomness and fluctuation. Figure 4b shows the probability distribution of the rotation frequency for tetramers and pentamers under the same condition. The ratio of average rotation frequency is the same as the inverse ratio of the trajectory perimeter as anticipated, but the clusters drifted in space. This is because they were buffeted not only by collisions with unattached active Janus particles but also by the imperfect rotational symmetry stemming from internal fluctuations around the average Janus–Janus envelope geometry. Though the underlying mechanism differs, it is noteworthy that the spatial trajectories of these rotors bear striking visual resemblance to some natural chiral microswimmers with motion driven by spiral-shaped flagellae (Figure 4c).[11]

Besides activity, the hub size in this system is crucial, not only concerning obvious geometrical packing, but also because range and strength of induced dipole moments scale with its volume. However, a sufficiently large size mismatch between hub and circumferential particles changes qualitatively the steady-state clusters that form. When the hub-to-Janus ratio reaches a large mismatch of 3 (hub particles 9 μm in diameter), the assembled structures are not unique; they take various forms and mostly do not rotate as tendencies to rotate are cancelled by balance of forces in these large structures (Figure S3). We have observed up to three shells of Janus particles in such cases, but only the first shell is attached rigidly, while particles in the second and third shells are transiently bonded to the cluster and exchange frequently with free Janus particles in the suspension.

In conclusion, clusters can be selected which differ from the most favorable configuration indicated by the energy landscape in an otherwise passive system. This is a truly non-equilibrium assembly scenario, in contrast to the traditional approach of perturbing equilibrium while maintaining the structures assembled from the same energetic interactions that control equilibrium self-assembly.[10b,12] The directed self-assembly requires energy input to deviate from the paths taken by a passive system. Furthermore, the design of such an active system can be subtle, in hope of utilizing the activity or energy input to guide the kinetic aspect of the assembly system. Our work with careful choice of the hub particle size and particle activity demonstrated this possibility, and even a controlled bifurcation with simple tuning of experimental parameters. Another example is a recent work[13] in which the authors intentionally choose the size ratio of a passive gear and active particles to guide the anchoring of active particles to the gear for the deterministic assembly of a micromachine device. Understanding and exploiting the new possibilities brought by the activity or autonomy of building blocks could open a new perspective and lead to more desired functionality in the field of directed self-assembly.

Acknowledgements

This work was supported at the University of Illinois by the US Department of Energy, Division of Materials Science, under award DE-FG02-07ER46471 through the Frederick Seitz Materials Research Laboratory. At the IBS Center for Soft and Living Matter, SG acknowledges support by the Institute for Basic Science, project code IBS-R020-D1.

Keywords: colloids · dynamic pathway · Janus particle · self-assembly · self-propelled particle

How to cite: *Angew. Chem. Int. Ed.* **2016**, *55*, 5166–5169
Angew. Chem. **2016**, *128*, 5252–5255

[1] I. Greving, M. Z. Cai, F. Vollrath, H. C. Schniepp, *Biomacromolecules* **2012**, *13*, 676–682.
[2] Y. S. Velichko, J. R. Mantei, R. Bitton, D. Carvajal, K. R. Shull, S. I. Stupp, *Adv. Funct. Mater.* **2012**, *22*, 369–377.
[3] J. Yan, M. Bloom, S. C. Bae, E. Luijten, S. Granick, *Nature* **2012**, *491*, 578–581.
[4] Y. Gao, J. F. Shi, D. Yuan, B. Xu, *Nat. Commun.* **2012**, *3*, 1033.
[5] M. Ballerini, N. Calbibbo, R. Candeleir, A. Cavagna, E. Cisbani, I. Giardina, V. Lecomte, A. Orlandi, G. Parisi, A. Procaccini, M. Viale, V. Zdravkovic, *Proc. Natl. Acad. Sci. USA* **2008**, *105*, 1232–1237.
[6] J. Wang, *ACS Nano* **2009**, *3*, 4–9.
[7] F. D. Ma, D. T. Wu, N. Wu, *J. Am. Chem. Soc.* **2013**, *135*, 7839–7842.
[8] a) T. M. Squires, M. Z. Bazant, *J. Fluid Mech.* **2006**, *560*, 65–101; b) S. Gangwal, O. J. Cayre, M. Z. Bazant, O. D. Velev, *Phys. Rev. Lett.* **2008**, *100*, 058302.
[9] a) P. García-Sánchez, Y. K. Ren, J. J. Arcenegui, H. Morgan, A. Ramos, *Langmuir* **2012**, *28*, 13861–13870; b) V. N. Shilov, A. V. Delgado, F. Gonzalez-Caballero, C. Grosse, *Colloids Surf. A* **2001**, *192*, 253–265.
[10] a) M. Mijalkov, G. Volpe, *Soft Matter* **2013**, *9*, 6376–6381; b) F. D. Ma, S. J. Wang, D. T. Wu, N. Wu, *Proc. Natl. Acad. Sci. USA* **2015**, *112*, 6307–6312.
[11] a) W. R. DiLuzio, L. Turner, M. Mayer, P. Garstecki, D. B. Weibel, H. C. Berg, G. M. Whitesides, *Nature* **2005**, *435*, 1271–1274; b) E. Lauga, W. R. DiLuzio, G. M. Whitesides, H. A. Stone, *Biophys. J.* **2006**, *90*, 400–412; c) L. Lemelle, J. F. Palierne, E. Chatre, C. Place, *J. Bacteriol.* **2010**, *192*, 6307–6308.
[12] a) W. Gao, A. Pei, X. M. Feng, C. Hennessy, J. Wang, *J. Am. Chem. Soc.* **2013**, *135*, 998–1001; b) F. C. Keber, E. Loiseau, T. Sanchez, S. J. DeCamp, L. Giomi, M. J. Bowick, M. C. Marchetti, Z. Dogic, A. R. Bausch, *Science* **2014**, *345*, 1135–1139.
[13] C. Maggi, J. Simmchen, F. Saglimbeni, J. Katuri, M. Dipalo, F. De Angelis, S. Sanchez, R. Di Leonardo, *Small* **2015**, *12*, 446–451.

Received: October 26, 2015
Revised: December 26, 2015
Published online: March 24, 2016

